Chapter 4
Biomechanical Modelling of Hierarchical Metamaterials for Skin Grafting

Vivek Gupta and Arnab Chanda

1 Introduction

The skin is mainly divided into three layers. The upper layer is called the epidermal layer, middle layer called dermal layer and bottom layer called hypodermal layer [1]. Skin performs several functions including preventing loss of moisture, reducing harmful effects of UV radiation and others [2]. There are several reasons which affect the skin properties such as electric stove heating, fires, accidents, cylinder explosions and many others [3]. The most common technique, which is used for burn injuries were full-thickness skin grafting (FTSG) and split-thickness skin grafting (STSG) [4–6].

Severe burns can be a devastating injury, often requiring extensive medical treatment to promote healing and prevent infection [3]. One crucial aspect of burn treatment is the use of skin grafts to cover damaged areas of skin [7]. However, due to the shortage of healthy skin, skin graft growth is a essential component of the healing process for large burn areas [8]. Skin grafting is the method of transplanting healthy skin from one region of the body to another to cover a wound or injury [2]. Full-thickness skin grafting (FTSG) and split-thickness skin grafting (STSG) are the two most common methods for skin grafting (STSG) [4–6]. In FTSG, the complete epidermis and dermis layer is removed from the abdomen. This technique is used for covering large burn areas and other wounds that require a thick, durable skin graft [9].

V. Gupta · A. Chanda (✉)
Centre for Biomedical Engineering, Indian Institute of Technology (IIT) Delhi, New Delhi, India
e-mail: arnab.chanda@cbme.iitd.ac.in

A. Chanda
Department of Biomedical Engineering, All India Institute of Medical Sciences (AIIMS) Delhi, New Delhi, India

A. Chanda et al. (eds.), *Materials for Biomedical Simulation*, Materials Horizons: From Nature to Nanomaterials, https://doi.org/10.1007/978-981-99-5064-5_4

STSG, on the other hand, includes removing only the epidermis and a part of the dermis from a healthy area of skin [9, 10]. This technique is often used for large burns due to its quicker healing time of 4–6 weeks [11, 12]. Additionally, STSG is frequently utilized for its ability to expand the skin graft by creating numerous parallel lines of small cuts on the intact removed skin using an appropriate skin grafting technique [2]. The skin grafting technique helps increase the capacity of STSG expansions, and the expansion is stated as a meshing ratio (MR) [13, 14]. Although several companies claim that STSGs can achieve skin expansions or meshing ratios of up to nine, clinical trials have shown that the highest expansion possible for STSG is just three [8, 15]. This emphasizes the importance of careful planning and management in skin grafting procedures, as well as the need for ongoing research to improve the effectiveness of burn treatments [16, 17].

Additive manufacturing (AM) techniques, mostly known as 3D printing, are being utilized to create skin graft patterns that can be tested using tensile testing machine. Gupta et al. [18] developed skin graft phantoms using AM techniques to determine the meshing ratios for low slit lengths and spacings. This allowed them to test and optimize skin graft designs before performing actual surgeries on patients. Javaid et al. [19] employed AM to design and create organ and scaffold components for tissue and organ printing. They found that 3D printing with scanned data could generate complex interior structures and could also be utilized to produce bone tissues for treating bone problems. Makode et al. [20] used two-part polymeric material, silicone, to fabricate skin simulant molds with matrix and collagen fiber oriented from 0° to 90°. By studying the variation in stress for several oriented skin simulants, they identified the best orientations for skin grafts. Baranski et al. [21] used a micropatterned polydimethylsiloxane (PDMS) template to align endothelial cells (ECs) within a collagen gel using AM. This allowed them to create complex vascular structures, which can be used to create clinically relevant heterogeneous tissue constructions. Vyas et al. [22] co-printed several cell-laden bio-inks to construct vasculature. This technique allows for the creation of complex and clinically relevant tissue structures.

Recently in 2022, Singh et al. [23] fabricated RT-shaped auxetic skin graft phantoms with varying angles of 0° to 135° using AM. In their study, they calculated stress, expansion, meshing ratio, and strain to identify the optimal design parameters for skin grafts. They concluded that skin grafts with a low RT angle would show maximum expansion. Overall, AM techniques are becoming an important tool in the design and testing of skin graft models. They allow for the creation of complex and customized structures that can be optimized for maximum effectiveness. By using these techniques, researchers can advance the field of skin grafting and improve outcomes for patients.

Wide-meshed skin grafts are often used to cover large areas of burn wounds and other skin injuries [24]. However, these grafts are usually weaker than normal skin due to the gaps in the mesh structure [25]. The mechanical strength of the graft depends on several factors, such as the type of mesh used and the technique used to attach the mesh to the wound bed [26]. To improve the mechanical strength of wide meshed skin grafts, various techniques have been developed [24, 27]. One of the approaches is to use an artificial dermis or dermal substitute to provide additional support for the mesh [28]. This can be achieved by placing a synthetic or biological material between the graft and the wound bed to promote tissue regeneration and healing [28]. Another approach is to use a modified mesh with a tighter structure or a different material composition to improve its strength. This modified mesh can be made of materials such as silicone or polyurethane, which are more durable and less prone to tearing [29]. In addition to these approaches, growth factors or other wound healing agents can be topically applied to the wound to improve tissue regeneration and wound healing. This can contribute to the overall strength of the graft [30].

There are two types of materials based on their Poisson's ratio: those with a positive Poisson's ratio and those with a negative Poisson's ratio [31]. The latter are referred to as auxetic materials, and they exhibit distinct characteristics from natural materials [32, 33]. Researchers have recently explored the use of auxetic patterns for designing skin grafts with better expansion potential [8, 23, 34]. For instance, Gupta et al. [34] investigated the effect of auxetic structures on the expansion potential of skin grafts and observed that these patterns had higher expansion than traditional ones. In a similar study, Gupta et al. [8] conducted a parametric analysis of various auxetic patterns with varying dimensional parameters and found that these structural changes could affect the axial change and expansion potential of the materials. Hierarchical auxetic structures with negative Poisson's ratio were found to exhibit higher strengths [35–37]. These structures are characterized by substructures with their geometry, allowing them to undergo multi-level deformation processes and exhibit unique mechanical behaviors. This approach mimics the natural environment to determine its role in strengthening materials and has been applied in various fields, including construction cranes and scaffolding [35–37].

The current study focuses on the development of hierarchical auxetic skin graft simulants, which can potentially improve burn surgery outcomes. The authors designed alternating slit (AS) and rotating rectangle (RR) shaped auxetic skin grafts using a design tool, and additive manufacturing was used to develop the molds. Silicone was then used to fabricate the hierarchical auxetic structures, which were evaluated for their expansion potential. The study estimated various parameters such as stress–strain, Poisson's ratio, meshing ratio, and void area. The modeling and testing methodologies used for skin graft simulants are discussed in Sect. 2, and the results are presented in Sect. 3, followed by the conclusions in Sect. 4. Overall, the study highlights the potential of hierarchical auxetic skin grafts as a promising approach for improving burn surgery outcomes.

2 Materials and Methods

2.1 Geometrical Modeling

CAD modelling was used to design the hierarchical patterns. The dimensions and schematic of all the designs was shown in Table 1 and Fig. 1 respectively. The dimensions of the designs were selected from the prior studies. Total four CAD models was designed using the 3D modelling software called SolidWorks (Dassault Systèmes, Vélizy-Villacoublay, France). For this study, the outer dimensions of the hierarchical patters were 50 mm × 50 mm × 2 mm. Figure 1 illustrates the first- and second-order AS and RR-shaped auxetic skin graft models. For the design of the first-order AS-shaped auxetic skin graft, the length of the alternating slits was retained the same as in earlier studies of AS-shaped and its derivatives. To investigate the influence of dimension parameters, the length of alternate slits in the first-order RR-shaped design was not equal. The number of slits was same in first-order AS and RR-shaped auxetic designs. The auxetic structures of the second-order hierarchy had more slits.

2.2 Fabrication of Skin Graft Simulants

The section outlines a method for producing a substance that efficiently mimics the epidermis and dermis at a depth of 2 mm (Fig. 2). The materials composition was produced applying a polymeric substance that has been utilized in comparable investigations on cadaveric skin and skin simulants. Several skin simulant pieces were produced and evaluated employing uniaxial stress at a 24 mm/min displacement rate, similar to previous studies [20, 38–41]. These compositions mechanical characteristics were compared to the mechanical properties of cadaver skin [42]. On the basis of the results of these experiments, an appropriate skin simulant composition was chosen. A polymeric material with a shore hardness of 5A was mixed with another polymeric material having a shore hardness of 30A in a weight ratio of 1:1. Pouring the compound into moulds with hierarchical auxetic patterns. The mixture was kept for 6 to 8 h to cure. The ultimate shore hardness of the skin graft simulants was 15A ± 2A, which was comparable to the qualities of cadaveric skin. In conclusion, the section presents a method for generating a polymeric composition

Table 1 Hierarchical skin graft model parameters, in millimetres

AS 1st order	H_1 or $L_1 = 17.92$	$H'_1 = 8.96$	$H''_1 = 4.48$	$T_{H1} = 11.2$
AS 2nd order	H_2 or $L_2 = 8.96$	$H'_2 = 4.48$	$H''_2 = 2.24$	$T_{H2} = 5.6$
RR 1st order	$X_1 = 8.96$	$L'_1 = 4.48$	$L''_1 = 4.48$	$T_{L1} = 11.2$
RR 2nd order	$X_2 = 4.48$	$L'_2 = 2.24$	$L''_2 = 2.24$	$T_{L2} = 5.6$

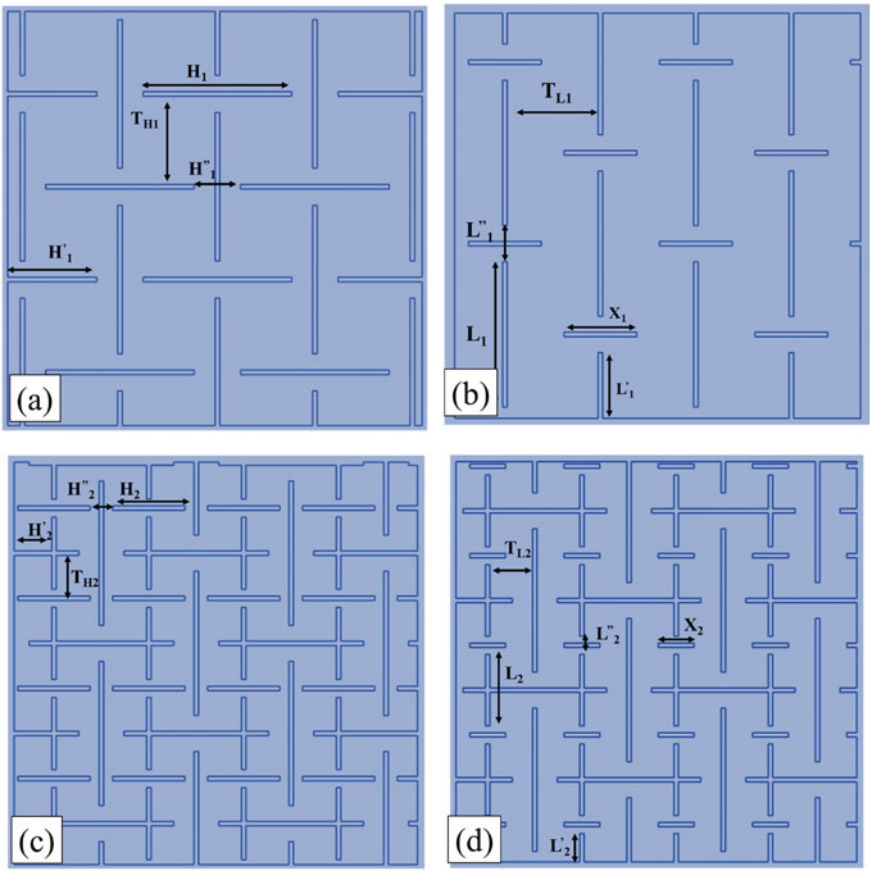

Fig. 1 Hierarchical auxetic skin graft designs **a** 1st order AS-shaped **b** 1st order RR-shaped **c** 2nd order AS-shaped **d** 2nd order RR-shaped

that replicates the the epidermis and 2 mm of dermis at medium depth. This composition was produced by repeated testing and comparison to cadaveric human skin, yielding a composition with a shore hardness comparable to that of cadaveric skin. After molding and curing the material, skin graft simulants were developed.

The process of developing 3D moulds for hierarchical skin grafts using additive manufacturing techniques. The dimensions of the moulds were consistent at 70 mm $\times$ 50 mm $\times$ 2 mm with an offset of 2 mm. The design and development of four skin graft moulds, each with a hierarchy of order up to two, was accomplished. Additive manufacturing process was used to process a 3D model, which is created using a computer-aided design (CAD) software, and then a 3D printer is used to print the model layer by layer [43–46]. In this case, the STL (STereoLithography) files of the moulds were converted into g-code and printed using a 3D printer that used Polylactic Acid (PLA) as a printing material. The printer was run with certain parameters, such

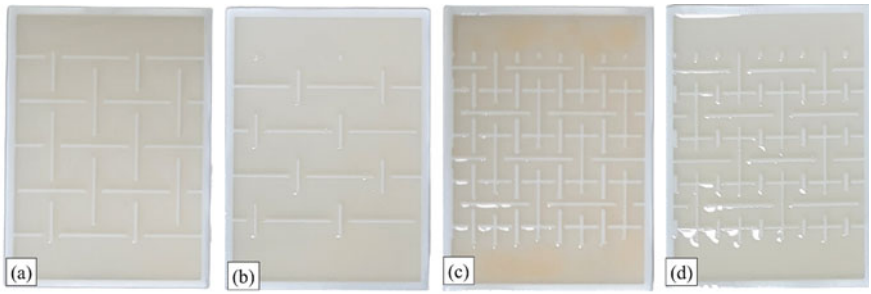

Fig. 2 Skin grafts with varying hierarchical moulds **a** 1st order AS-shaped **b** 1st order RR-shaped **c** 2nd order AS-shaped **d** 2nd order RR-shaped

as a nozzle temperature of 210 °C, a bed temperature of 60 °C, a printing speed of 45 mm/sec, and a layer height of 0.1 mm. When the moulds had been produced, the skin graft simulants were cast using these moulds.

2.3 Mechanical Testing

A universal testing machine (UTM) commonly utilized for material characterization under uniaxial loading conditions. In this work, four hierarchical auxetic patterns were tested under uniaxial tensile condition. In UTM, the sample was attached tightly with the clamps and one clamp was attached with the load cell. As the UTM is functional, the upper clamp was moving and sample stretched. All these experiments were performed at constant speed of 0.4 mm/sec. The schematic of sample attachment and load cell was shown in Fig. 3. The force–displacement data was converted into stress(σ)-strain (ε) data using the Eq. 1. The Poisson's ratio of all the hierarchical patterns was calculated using Eq. 2, under different stretching conditions. However, it was noted that the effective Poisson's ratio changes with the type of materials used. To determine the longitudinal strain, the maximum displacement that could be delivered in the direction of the uniaxial loading was divided by the hierarchical skin graft simulant initial length (L). Using Eq. 3, we were able to determine the lateral strain by dividing the maximal orthogonal displacement by the width of the graft model at the beginning of the calculation. The meshing ratio (MR) was measured during the uniaxial testing to determine the expansion of the skin graft simulants. The MR was defined as the expanded area of the skin graft to the unexpanded area of the skin graft, using Eq. 4. Void area is crucial parameters for cellular proliferation in developing cells. Void area. In this skin grafting work, the void area, which refers to an area that is empty or contains nothing, is extremely crucial. Using imaging methods, the empty area and maximum edge length were computed by determining the maximum value of X and Y. In summary, the methods used to perform uniaxial testing on hierarchical auxetic skin graft simulants using a UTM. The force–displacement data

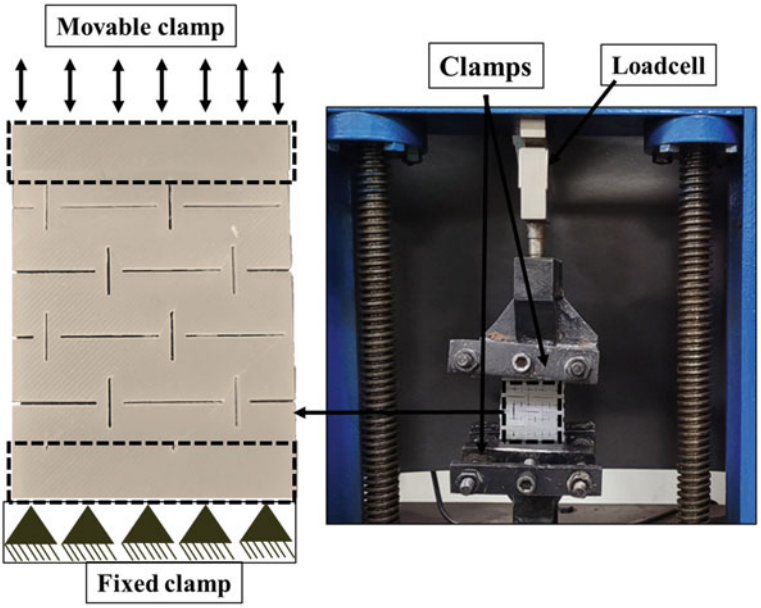

Fig. 3 Uniaxial testing configuration for skin graft simulators on the UTM

obtained from the UTM were converted to stress–strain. The effective Poisson's ratio, longitudinal strain, and lateral strain were estimated using Eqs. 1–3. The expansion of the skin graft simulants was measured using the meshing ratio, as defined by Eq. 4.

$$\text{Stress } (\sigma) = \frac{\text{Force (F)}}{\text{Cross}-\text{section area (A)}}, \tag{1}$$

$$\text{Poissons ratio } (\nu_{12}) = -\frac{d\varepsilon_2}{d\varepsilon_1}, \tag{2}$$

where $d\varepsilon_1, d\varepsilon_2$ are the longitudinal and lateral strain.

$$d\varepsilon_1 = \frac{d\mathrm{L}_1}{\mathrm{L}_1} \; and \; d\varepsilon_2 = \frac{d\mathrm{L}_2}{\mathrm{L}_2}, \tag{3}$$

$$\mathrm{MR} = \frac{\text{Expanded Area}}{\text{Unexpanded Area}}. \tag{4}$$

3 Results and Discussion

3.1 Stress Analysis of Hierarchical Auxetic Skin Graft Simulants

Figure 4 illustrates the stress–strain values of hierarchical auxetic patterns at different stretching levels up to 300%. 1st order RR shaped patterns shows the maximum stress values and 2nd order AS shaped auxetic pattern shows the minimum stress values. The maximum and minimum stress value was 145 kPa and 85 kPa. It was observed that up to 20% strain, the stress values in all the hierarchical model was very low. Similar work conducted by the Gupta et al. [18], in their work, oval shape skin graft patterns was fabricated with varying dimensional parameters and calculated stress values were under the same range. From the stress analysis, 2nd order AS shaped hierarchical auxetic skin graft simulant shows the minimum stress value and could be best combination for skin grafting technique. It is emphasized that the lowest stress obtained in the study indicates the less chances of rupture of a hierarchical auxetic skin graft simulant.

3.2 Poisson's Ratio Analysis of Hierarchical Auxetic Skin Graft Simulants

The results of Poisson's ratio analysis for hierarchical auxetic skin graft simulants, as shown in Fig. 5. The Poisson's ratio values were calculated at 100%, 200%, and 300% strain. The negative Poisson's ratio values decreased for all skin graft models from 100 to 300% strain. At 100% strain, the 2nd order AS-shaped and 1st order RR-shaped auxetic skin graft simulant showed the highest and lowest negative Poisson's ratios (− 1.7 and − 1.5), respectively. Similarly, at 200% and 300% strains, the 2nd

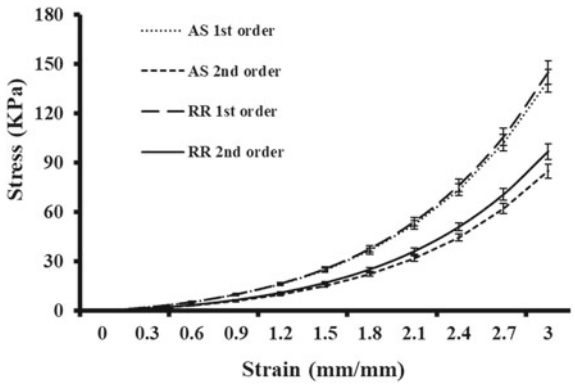

Fig. 4 Stress–strain plot of hierarchical auxetic skin graft simulants up to 300% strain

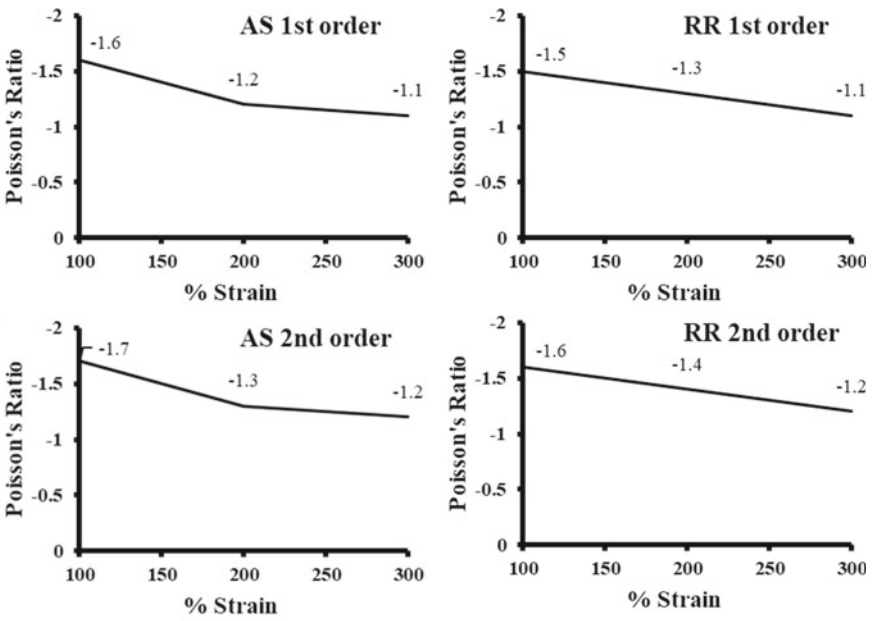

Fig. 5 Poisson's ratio of hierarchical auxetic skin graft simulants

order AS-shaped auxetic skin graft simulant and the 1st order RR-shaped auxetic skin graft simulant exhibited the highest and lowest negative Poisson's ratios, respectively. Overall, the hierarchical structures in this study showed negative Poisson's ratio values, and the 2nd order AS-shaped auxetic structure exhibited the highest Poisson's ratio. Based on these results, this structure may be the most suitable skin graft structure for covering large burn areas.

3.3 Meshing Ratio Analysis of Hierarchical Auxetic Skin Graft Simulants

Figure 6 illustrates the meshing ratio (MR) of the hierarchical auxetic skin graft simulants up to their ultimate tensile strength (UTS). The study conducted five tests on each of the skin graft models to ensure repeatability of the data. The results indicated that stretching caused an increase in the MR values of the hierarchical structures. At 100%, 200%, 300% strain, and UTS elongation, the 2nd order RR-shaped skin graft simulant exhibited the lowest MR values, whereas the 1st order AS-shaped patterns showed the highest MR values. The 1st order AS-shaped auxetic skin graft simulant had a maximum MR value of 5.8, while the 2nd order RR-shaped had the minimum MR value of 5 at UTS. The other two hierarchical skin graft simulants, namely the 2nd order AS-shaped and the 1st order RR-shaped, showed

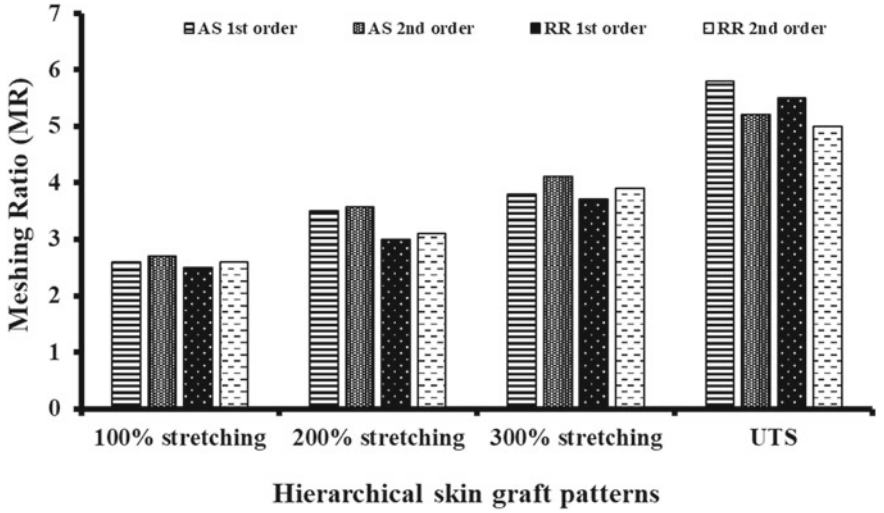

Fig. 6 Uniaxial meshing ratios for hierarchical auxetic skin graft simulants

MR values of 5.2 and 5.5, respectively. Therefore, the skin graft covering the largest area with cell growth and other clinical aspects will be the most appropriate for skin grafting applications and will cover extensive burn areas. The meshing ratio value can provide insights into the strength and structural integrity of the skin graft, which is crucial for ensuring its success in covering and protecting burn areas.

3.4 Void Area Analysis of Hierarchical Auxetic Skin Graft Simulants

The void area of hierarchical auxetic skin graft patters of each unit cell at different levels was shown in Table 2. The void area, which represents the space between the unit cells, is a crucial parameter affecting the skin ability to regenerate and heal. Higher void areas can impede cell proliferation, leading to reduced graft success rates and poor wound healing. However, biological investigations, such as studies with cadaveric and animal skins and healing agents, are needed to estimate cell proliferation and wound healing in these designs. Overall, the 1st order RR-shaped skin graft simulants showed a higher void area compared to the all other skin graft models. 2nd order AS-shaped skin graft simulants shows the minimum void area. Overall The results suggest that the 2nd order AS-shaped hierarchical auxetic skin graft designs coude be the best possible graft, which is used in skin grafting applications.

Table 2 Void area values of different hierarchical patterns

Design	Initial void area (mm^2)	Void area at 100% (mm^2)	Void area at 200% (mm^2)	Void area at 300% (mm^2)
AS 1st order	35.84	167	260	427
AS 2nd order	35.84	186	243	392
RR 1st order	35.84	183	226	463
RR 2nd order	35.84	181	221	459

4 Conclusions

This work details an experimental investigation into the biomechanics of hierarchical skin graft simulants. To develop skin graft simulants, AS- and RR-shaped auxetic patterns with distinct levels of hierarchy were developed. 3D printing techniques were utilized to manufacture moulds for the biofidelic material that replicates the mechanical properties of human skin. Uniaxial tensile experiments were conducted to evaluate the stress caused by hierarchical structures on skin graft simulants. Poisson's ratio, meshing ratio and void area was calculated to understand the maximum expansion and maximum void reign after stretching. At maximum tensile strength, the 2nd AS shaped auxetic skin graft simulant displayed the minimum indused stress, maximum Poisson's ratio and minimum void region, greatest meshing ratio (UTS). Overall, the 2nd order AS-shaped auxetic skin graft simulant was the most stable design for expansion without the risk of skin rupture. Also, this study provides insight into the biomechanics of hierarchical skin graft simulants and demonstrates the potential for expanding skin grafts using auxetic patterns. The findings suggest that such an approach may be a promising avenue for improving the outcomes of burn surgery.

References

1. Singh G, Chanda A (2021) Mechanical properties of whole-body soft human tissues: a review. Biomed Mater 16(6):062004. https://doi.org/10.1088/1748-605X/AC2B7A
2. Capek L, Flynn C, Molitor M, Chong S, Henys P (2018) Graft orientation influences meshing ratio. Burns 44(6):1439–1445. https://doi.org/10.1016/J.BURNS.2018.05.001
3. MacNeil S (2007) Progress and opportunities for tissue-engineered skin. Nature 445(7130):874–880. https://doi.org/10.1038/nature05664
4. Narayan N, Shivaiah R, Kumar KM (2021) A novel technique of collagen application over meshed split thickness graft for wound coverage. Int J Surg Med 7:54–61. https://doi.org/10.5455/ijsm.Collagen-Application-Meshed-Split-Thickness-Graft
5. Bogdanov SB, Gilevich IV, Melkonyan KI, Sotnichenko AS, Alekseenko SN, Porhanov VA (2021) Total full-thickness skin grafting for treating patients with extensive facial burn injury: a 10-year experience. Burns 47(6):1389–1398. https://doi.org/10.1016/j.burns.2020.12.003
6. Noureldin MA, Said TA, Makeen K, Kadry HM (2022) Comparative study between skin micrografting (Meek technique) and meshed skin grafts in paediatric burns. Burns 48(7):1632–1644. https://doi.org/10.1016/j.burns.2022.01.016

7. Hosseini M, Shafiee A (2021) Engineering bioactive scaffolds for skin regeneration. Small 17(41):2101384. https://doi.org/10.1002/smll.202101384
8. Gupta V, Chanda A (2022) Expansion potential of skin grafts with alternating slit based auxetic incisions. Forces Mech 7:100092. https://doi.org/10.1016/J.FINMEC.2022.100092
9. Claeys S (2017) Skin grafting. In: Griffon D, Hamaide A (eds) Complications in small animal surgery. StatPearls Publishing, Chichester, pp 561–568
10. Kagan RJ et al (2013) Surgical management of the burn wound and use of skin substitutes: an expert panel white paper. J Burn Care Res 34(2):e60–e79. https://doi.org/10.1097/BCR.0b013e31827039a6
11. Fan R, Hao R, McCarthy A, Xue J, Chen S (2023) Skin involved nanotechnology. In: Ning G (ed) Nanomedicine. Springer, Singapore, pp 719–753. https://doi.org/10.1007/978-981-16-8984-0_31
12. Zhou J, Scott C, Miab ZR, Lehmann C (2023) Current approaches for the treatment of ketamine-induced cystitis. Neurourol Urodyn 42(3):680–689. https://doi.org/10.1002/nau.25148
13. Huri D, Mankovits T (2018) Comparison of the material models in rubber finite element analysis. IOP Conf Ser Mater Sci Eng 393(1):012018. https://doi.org/10.1088/1757-899X/393/1/012018
14. Ozhathil DK, Tay MW, Wolf SE, Branski LK (2021) A narrative review of the history of skin grafting in burn care. Medicina 57(4):380. https://doi.org/10.3390/medicina57040380
15. Vandeput J, Nelissen M, Tanner JC, Boswick J (1995) A review of skin meshers. Burns 21(5):364–370. https://doi.org/10.1016/0305-4179(94)00008-5
16. Tang Y, Yin J (2017) Design of cut unit geometry in hierarchical kirigami-based auxetic metamaterials for high stretchability and compressibility. Extrem Mech Lett 12:77–85. https://doi.org/10.1016/J.EML.2016.07.005
17. Payne T, Mitchell S, Bibb R, Waters M (2014) Initial validation of a relaxed human soft tissue simulant for sports impact surrogates. Procedia Eng 72:533–538. https://doi.org/10.1016/j.proeng.2014.06.092
18. Gupta V, Chanda A (2022) Biomechanics of skin grafts: effect of pattern size, spacing and orientation. Eng. Res. Express 4(1):015006. https://doi.org/10.1088/2631-8695/AC48CB
19. Javaid M, Haleem A (2020) 3D printed tissue and organ using additive manufacturing: an overview. Clin Epidemiol Glob Heal 8(2):586–594. https://doi.org/10.1016/J.CEGH.2019.12.008
20. Makode S, Singh G, Chanda A (2021) Development of novel anisotropic skin simulants. Phys Scr 96(12):125019. https://doi.org/10.1088/1402-4896/AC2EFD
21. Baranski JD et al (2013) Geometric control of vascular networks to enhance engineered tissue integration and function. Proc Natl Acad Sci USA 110(19):7586–7591. https://doi.org/10.1073/PNAS.1217796110/SUPPL_FILE/PNAS.201217796SI.PDF
22. Vyas C, Pereira R, Huang B, Liu F, Wang W, Bartolo P (2017) Engineering the vasculature with additive manufacturing. Curr Opin Biomed Eng 2:1–13. https://doi.org/10.1016/j.cobme.2017.05.008
23. Singh G, Gupta V, Chanda A (2022) Mechanical characterization of rotating triangle shaped auxetic skin graft simulants. Facta Univ Ser Mech Eng. https://doi.org/10.22190/FUME220226038S
24. Shree A, Vagga AA (2022) Methodologies of autologous skin cell spray graft. Cureus. https://doi.org/10.7759/cureus.31353
25. Cigna E, Bolletta A, Giardino FR, Patanè L (2022) Grafts in plastic surgery. In: Maruccia M, Giudice G (eds) Textbook of plastic and reconstructive surgery. Springer, Cham, pp 61–75
26. Radharaman P, Kumar AKS, Kumar Sharma R (2019) The role of recruited minced skin grafting in improving the quality of healing at the donor site of split-thickness skin graft—A comparative study. Burns 45(4):923–928. https://doi.org/10.1016/j.burns.2018.11.018
27. Noor A et al (2022) Dressings for burn wound: a review. J Mater Sci 57(12):6536–6572. https://doi.org/10.1007/s10853-022-07056-4
28. Mandal BB, Kapoor S, Kundu SC (2009) Silk fibroin/polyacrylamide semi-interpenetrating network hydrogels for controlled drug release. Biomaterials 30(14):2826–2836. https://doi.org/10.1016/J.BIOMATERIALS.2009.01.040

29. Bell MA, Becker KP, Wood RJ (2022) Injection molding of soft robots. Adv Mater Technol 7(1):2100605. https://doi.org/10.1002/admt.202100605
30. Kaur G, Narayanan G, Garg D, Sachdev A, Matai I (2022) Biomaterials-based regenerative strategies for skin tissue wound healing. ACS Appl Bio Mater 5(5):2069–2106. https://doi.org/10.1021/acsabm.2c00035
31. Ren X, Das R, Tran P, Ngo TD, Xie YM (2018) Auxetic metamaterials and structures: a review. Smart Mater Struct. https://doi.org/10.1088/1361-665X/aaa61c
32. Liu Y, Hu H (2010) A review on auxetic structures and polymeric materials. Sci Res Essays 5(10):1052–1063
33. Shukla S, Behera BK (2022) Auxetic fibrous materials and structures in medical engineering—a review. Bioeng Transl Med. https://doi.org/10.1080/00405000.2022.2116549
34. Gupta S, Gupta V, Chanda A (2022) Biomechanical modeling of novel high expansion auxetic skin grafts. Int. J Numer Method Biomed Eng 38(5):3586. https://doi.org/10.1002/cnm.3586
35. Dudek KK, Martínez JAI, Ulliac G, Kadic M (2022) Micro-scale auxetic hierarchical mechanical metamaterials for shape morphing. Adv Mater 34(14):2110115. https://doi.org/10.1002/adma.202110115
36. Dudek KK et al (2017) On the dynamics and control of mechanical properties of hierarchical rotating rigid unit auxetics. Sci Rep 7(1):1–9. https://doi.org/10.1038/srep46529
37. Han DX, Chen SH, Zhao L, Tong X, Chan KC (2022) Architected hierarchical kirigami metallic glass with programmable stretchability. AIP Adv 12(3):8–13. https://doi.org/10.1063/5.0084906
38. Chanda A, Upchurch W (2018) Biomechanical modeling of wounded skin. J Compos Sci. https://doi.org/10.3390/jcs2040069
39. Gupta V, Chanda A (2023) Expansion potential of novel skin grafts simulants with I-shaped auxetic incisions. Biomed Eng Adv 5:100071. https://doi.org/10.1016/J.BEA.2023.100071
40. Singh G, Gupta V, Chanda A (2022) Artificial skin with varying biomechanical properties. Mater Today Proc 62:3162–3166. https://doi.org/10.1016/J.MATPR.2022.03.433
41. Gupta V, Singh G, Chanda A (2023) High expansion auxetic skin graft simulants for severe burn injury mitigation. Eur Burn J 4(1):108–120. https://doi.org/10.3390/EBJ4010011
42. Gallagher AJ, Ní Anniadh A, Bruyere K, Otténio M, Xie H, Gilchrist MD (2012) Dynamic tensile properties of human skin. International Research Council on the Biomechanics of Injury
43. Singh G, Chanda A (2023) Biofidelic gallbladder tissue surrogates. Adv Mater Process Technol. https://doi.org/10.1080/2374068X.2023.2198835
44. Singh G, Chanda A (2023) Development and biomechanical testing of artificial surrogates for vaginal tissue. Adv Mater Process Technol. https://doi.org/10.1080/2374068X.2023.2198837
45. Singh G, Chanda A (2023) Development and mechanical characterization of artificial surrogates for brain tissues. Biomed Eng Adv 5:100084. https://doi.org/10.1016/J.BEA.2023.100084
46. Gupta V, Singh G, Chanda A (2023) Development of novel hierarchical designs for skin graft simulants with high expansion potential. Biomed Phys Eng Express 9(3):035024. https://doi.org/10.1088/2057-1976/ACC661